Electronic Supplementary Material (ESI) for Journal of Materials Chemistry A.

Electronic Supplementary Information

Piperazine Diffusion Reduced Interfacial Polymerization for Ultrahigh permeable Nanofiltration Membranes via Nanofibrous Hydrogel

Shushan Yuan[#a,b], Gang Zhang [#a], Junyong Zhu [c], Natalie Mamrol [d], Suilin Liu [a], Zhaohuan Mai[*e], Peter Van Puyvelde [b], Bart Van der Bruggen*[b]

Contents

1 Methods

1.1 Materials

Bulk Kevlar 69 was purchased from Thread Exchange (USA) and was dried in an oven for 12 h at 60 °C before use. Potassium hydroxide (KOH, 85%), dimethyl sulfoxide (DMSO) and n-hexane (99%) were purchased from Sigma-Aldrich BVBA and used as received. Monomers used for interfacial polymerization including piperazine (PIP, 99%) and trimesoyl chloride (TMC, 98%) were purchased from Sigma- Aldrich (Diegem, Belgium). Four salts, sodium sulfate (Na_2SO_4, 99%), sodium chloride (NaCl, 99%), magnesium chloride ($MgCl_2$) and magnesium sulfate ($MgSO_4$, 99%), were purchased from Sigma-Aldrich and tested separately for salt rejection with 1.0 g/L of feed concentration.

1.2 Membrane synthesis

Nanofibrous hydrogel support membrane PIP saturated aqueous solution

A dark red Kevlar solution was prepared by stirring the mixture of bulk Kevlar 69 (2 g, from Thread Exchange, right twist), KOH (2 g), and dimethyl sulfoxide (DMSO, 100 ml) for 1 week at room temperature. Then, to make the hydrogel membrane, the Kevlar solution was cast onto a glass plate by a casting knife with a gap of 200 µm at room temperature with a humidity of 50–60%. The glass plate with Kevlar solution was subsequently immersed in an aqueous solution bath containing a certain concentration of PIP monomers (0.01 wt%-0.04 wt%). In this process, the exchange between DMSO in Kevlar solution and PIP aqueous solution lead to the formation of Kevlar hydrogel and preloading of the PIP monomers in the polymer network.

Interfacial polymerization on nanofibrous Kevlar hydrogel

In a typical thin composite membrane fabrication process, the polymeric membrane was first rinsed with PIP solution to deposit PIP monomers on the surface of the membrane, and then to induce the polymerization by pouring the TMC n-hexane solution on the PIP loaded nanofibrous hydrogel. In this experiment, the step of rinsing the support membrane with PIP monomers solution is not necessary because the hydrogel membrane is already preloaded with PIP monomers during the hydrogel formation, which greatly simplifies the membrane fabrication process. Therefore, the interfacial polymerization was directly conducted by dropping 6 ml of TMC n-hexane solution (1 mg ml^{-1}) on the bottom surface of hydrogel membrane. After reaction for 1 min, the excess TMC solution was removed and the membrane was then oven-cured at 60 °C for 6 mins. The obtained membranes were stored in deionized water for use.

Interfacial polymerization on conventional PSU ultrafiltration membrane

PSU-TFC membranes were synthesized via a conventional interfacial polymerization process. In brief, the support PSU ultrafiltration membrane was first wetted by 6 ml of PIP solution (0.01 wt%-0.1 wt%) for 5 min. The excess PIP solution was gently removed by compressed air until no water spots can be observed. Then, TMC n-hexane solution (1 mg ml^{-1}) was poured on the surface of the PSU membrane for the polymerization. After 1 min, the TMC n-hexane solution was removed and the membrane was put in the oven for 6 min at 60 °C. The obtained membranes were stored in deionized water for use.

Interfacial polymerization at free hexane/water interface for freestanding PA membranes

The free-standing membranes were synthesized using the methods reported by Zhu.[1] To achieve an interfacial polymerization of 1 min at the free aqueous-organic interface, the experiment was specifically designed. Before the interfacial polymerization, we measured that it takes 30 s for 5 ml of piperazine solution to go through the hydrogel supporting membrane. Then, 5 ml of PIP monomer solution (0.01 wt%-0.04 wt%) was poured in a vacuum filtration container where a Kevlar hydrogel membrane was positioned at the flat bottom. Afterwards, n-hexane solution containing TMC (1 mg ml^{-1}) was added gently using a pipette. After interfacial polymerization for 30 seconds, the aqueous solution was filtered through the Kevlar hydrogel membrane (it takes 30 s), while the PA layer was deposited on the surface of the Kevlar hydrogel membrane. After 1 min of interfacial polymerization, the organic solution was removed from the membrane surface. The resulting membrane was then put in the oven for 3 min at 70 °C to improve the stability between the PA nanofilm and the substrate. The obtained membranes were stored in deionized water for use.

Synthesis of Poly(vinyl alcohol) (PVA) based Hydrogel-TFC membrane

Preparation of PVA hydrogel membrane: PVA dope solution was prepared by dissolving 1.5 g PVA in 15 ml of 0.5 mol L^{-1} H_2SO_4 at 85 °C with magnetic stirring. Then, to make the PVA hydrogel membrane, the PVA solution was cast onto a glass plate by a casting knife with a gap of 200 µm at room temperature with a humidity of 50–60%. A nonwoven saturated with diluted 0.05 wt% glutaraldehyde (GA) solution was then covered on the surface of PVA solution film to cross link the PVA. After reacting for 10 min, nonwoven supported PVA hydrogel is formed and peeled from the glass plate. The hydrogel was then put in water to remove the unreacted residual chemicals.

Interfacial polymerization: PVA Hydrogel-TFC membranes were synthesized via a conventional interfacial polymerization process. In brief, the PVA hydrogel was first wetted by 6 ml of PIP solution (0.02 wt%) for 10 min. The excess PIP solution was gently removed by compressed air until no obvious water spot can be observed. Then, TMC hexane solution (1 mg ml^{-1}) was poured on the surface of the PVA hydrogel for the polymerization. After 1 min, the TMC hexane solution was removed and the membrane was put in the oven for 6 min at 60 °C. The obtained membranes were stored in deionized water for use.

1.3 Characterizations

SEM images were obtained from a Philips Scanning Electron Microscope XL30 FEG (the Netherlands) at 10 kV. The roughness of the membrane surface was obtained from a Dimension 3100 Atomic force microscope. TEM images were acquired from JEOL-1230 field-emission transmission electron microscopy. The chemical composition of the membrane surface was surveyed by an X-ray photoelectron spectroscopy (XPS, AXIS Supra, Kratos Analytical, UK) with a monochromatic Al Kα excitation source and analyzed by CasaXPS software. The surface charge of the hydrogel-TFC membranes was detected using a streaming potential method by an electro-kinetic analyzer (SurPASS 3, Anton Paar, Austria) with 1 mM NaCl solution as an electrolyte solution. Water contact angles were measured on a Data-Physics OCA 20 with 2 µl water droplet.

Water content of nanofibrous hydrogel

The water content of the hydrogels was calculated based on the weight of hydrogel (m_1) and dry hydrogel (m_2) by using the following equation:

$$Water\ content\ \% = \frac{m_1 - m_2}{m_1} \times 100\%$$

Membrane desalination measurement

A cross-flow setup was employed to measure the performance of nanofiltration membranes at a pressure of 4 bar. The effective area was 22.9 cm^2. The flux J is calculated using the following equation:

$$J = \frac{V}{A \times t}$$

where V (L) is the permeate volume, A (m^2) is the effective membrane area, t is the permeation time (h).

The permeance (L/m^2 h bar) is defined as the flux per unit applied pressure and can be calculated using the following equation:

$$P = \frac{J}{\Delta P}$$

where Q is the flow rate (L h^{-1}), ΔP is the trans-membrane pressure (bar) and A is the effective filtration area (m^2).

The salt rejection of nanofiltration membranes was calculated from the concentrations of salt at the feed and permeate by using the following equation:

$$R = \left(1 - \frac{C_p}{C_r}\right) \times 100\%$$

where C_p and C_r are salt concentration in the permeate and feed, respectively.

Supercritical drying

In order to preserve the macro-structure of nanofibrous Kevlar hydrogel membrane samples, supercritical CO_2 drying was applied. The details about the supercritical CO_2 drying process are as follows: Before the drying process, the water in hydrogel membranes was replaced with isopropanol. Thus, hydrogel membranes were firstly immersed in isopropanol for 2 h for the exchange of water. Then hydrogel membranes were taken out and were immersed in new pure isopropanol for another 2 h. This process was repeated 3 times to gradually replace the water with isopropanol. Finally, nanofibrous hydrogel membranes were placed in the supercritical point dryer for 1 h to obtain dry membranes.

2 Supplementary figures and tables

2.1 Nanofibrous Kevlar hydrogel

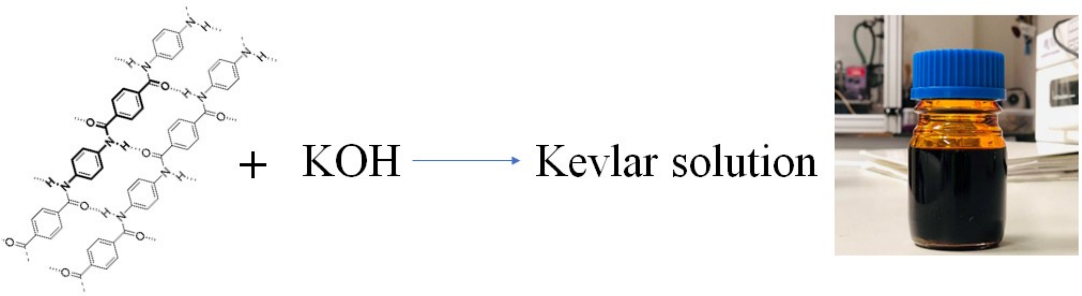

Figure S1 Kevlar/DMSO solution prepared by dissolving 2 g Kevlar and 2 g KOH in 100 g DMSO

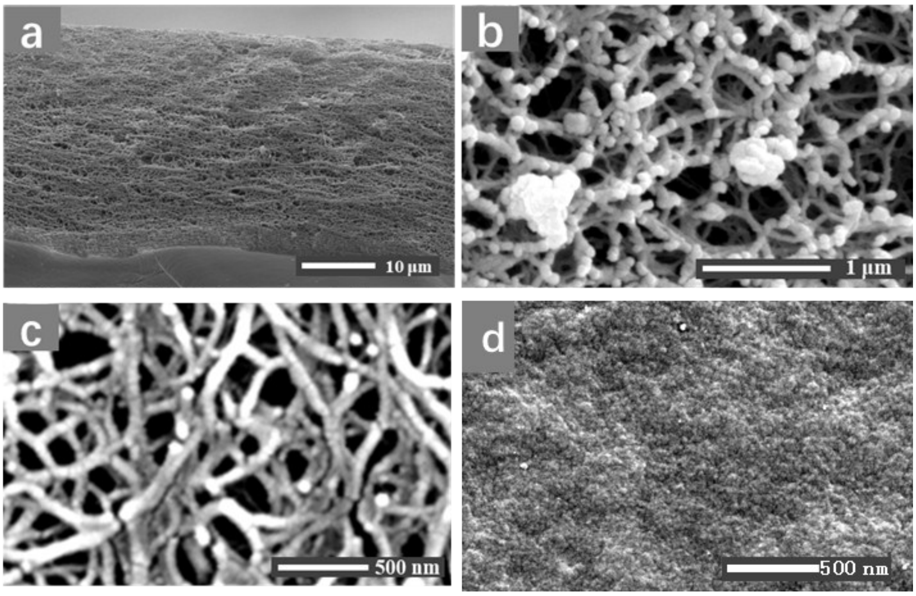

Figure S2 Cross-section (a), magnified cross-section (b), bottom surface (c) and top surface (d) of the hydrogel dried by a supercritical dryer.

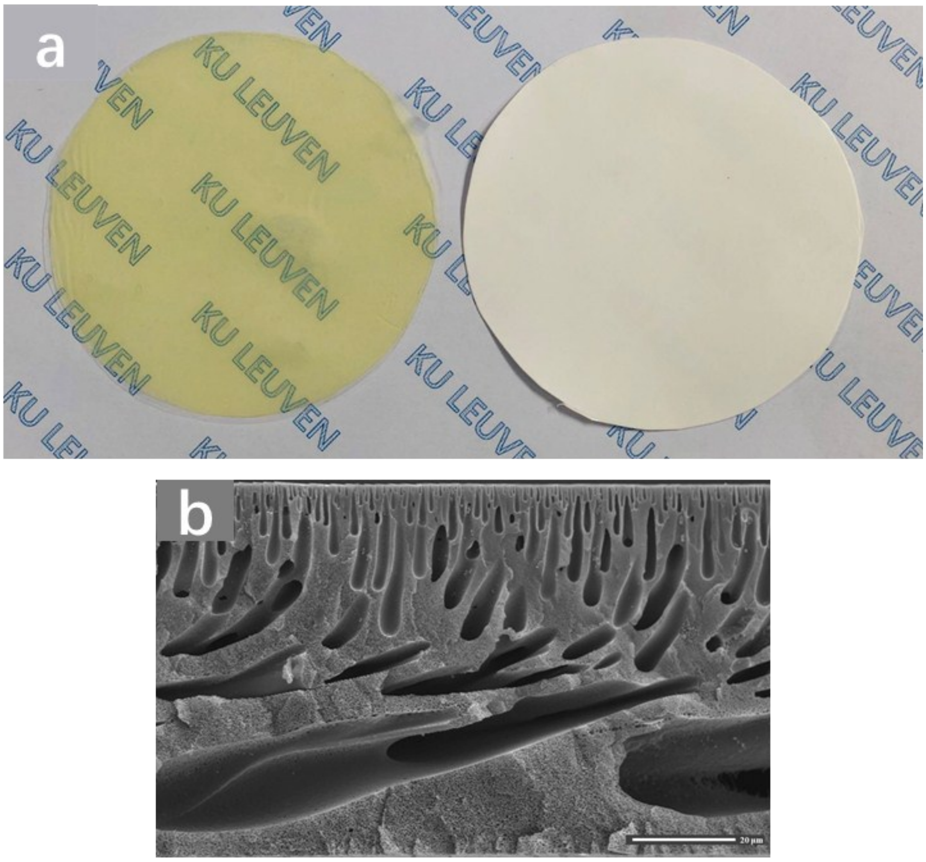

Figure S3 Comparation of convention polymeric membrane with nanofibrous hydrogel. a, the photograph of hydrogel (left) and conventional polymeric membrane (PSU, right) obtained from phase inversion; b, Cross-section morphology of conventional polymeric membrane (PSU) SEM image.

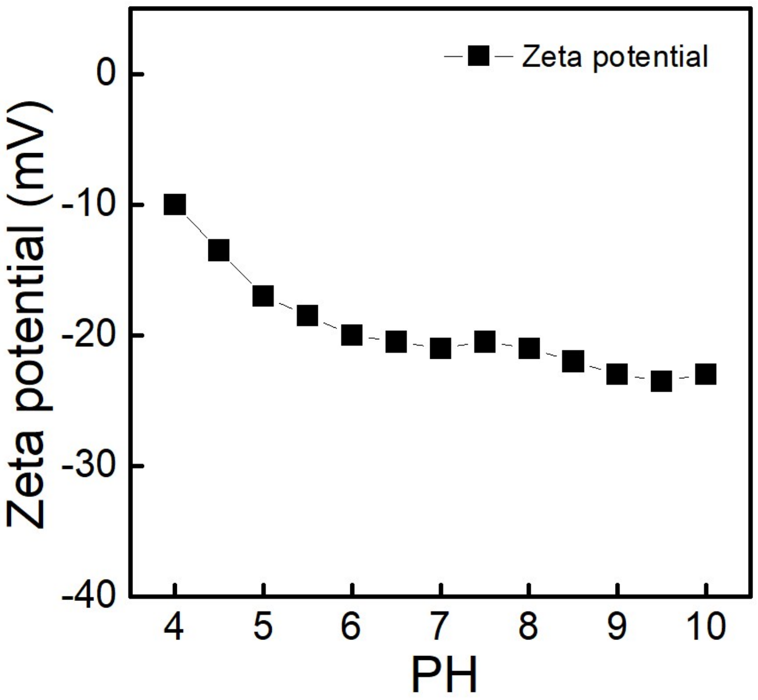

Figure S4 Zeta potential of nanofibrous Kevlar hydrogel membrane.

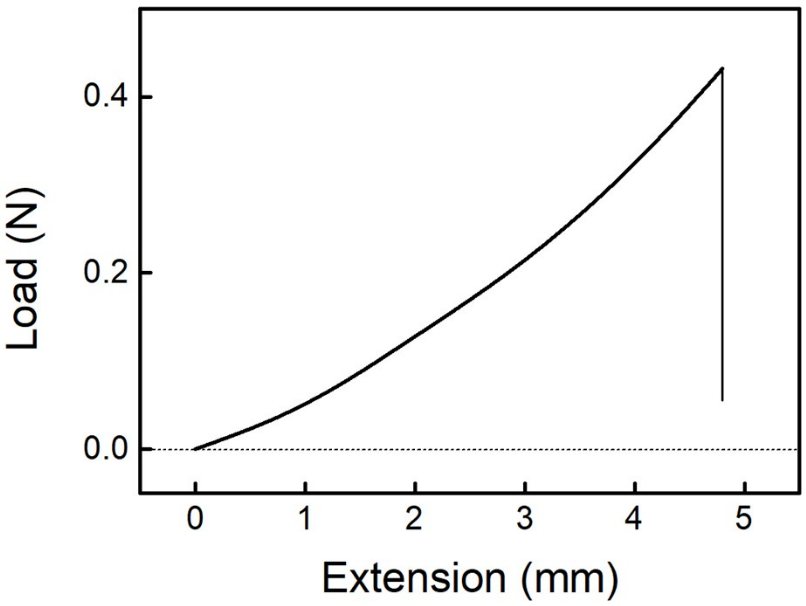

Figure S5 Mechanical strength of Kevlar support membrane. (Sample, width 3 mm, thickness 80 um, length 5 cm. 5 samples were tested; the average tensile strength of the nanofibrous hydrogel membrane is calculated as 0.185± 0.021 MPa).

2.2 Hydrogel-TFC membranes, PSU-TFC membranes, and freestanding PA membranes

Hydrogel-TFC membranes

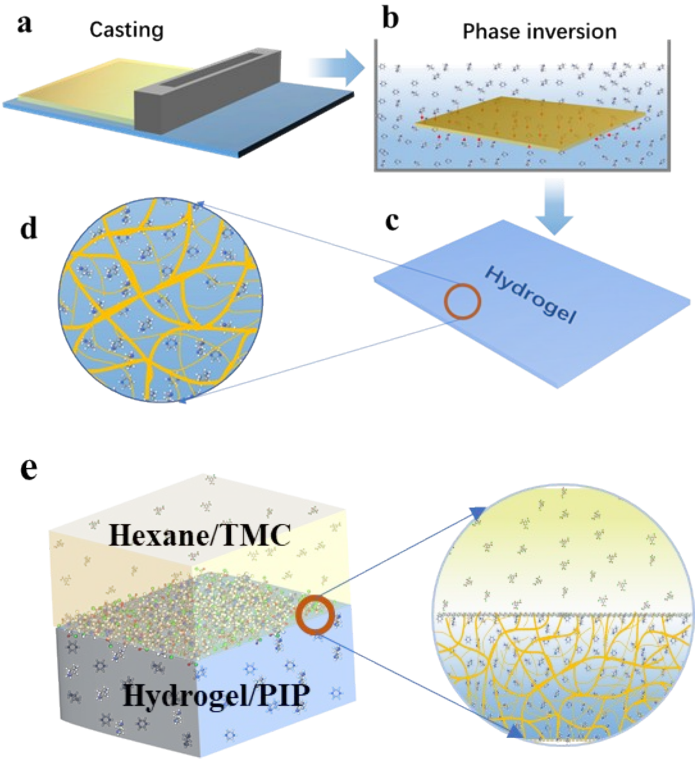

Figure S6 Scheme of synthesizing hydrogel-TFC membrane. (a) casting of Kevlar/DMSO (2 wt%) on a glass plate; (b) immersion of glass plates with Kevlar solution in water/PIP bath for phase inversion and preloading of PIP monomers in Kevlar hydrogel; (c) Kevlar hydrogel containing PIP monomers; (d) nanofibrous structures in hydrogel; (e) Interfacial polymerization to form hydrogel-TFC membrane.

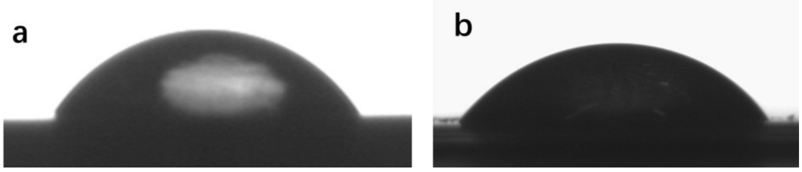

Figure S7 Water contact angle of dry nanofibrous hydrogel (72°) and Hydrogel-TFC membrane (PIP-0.015， 54°)

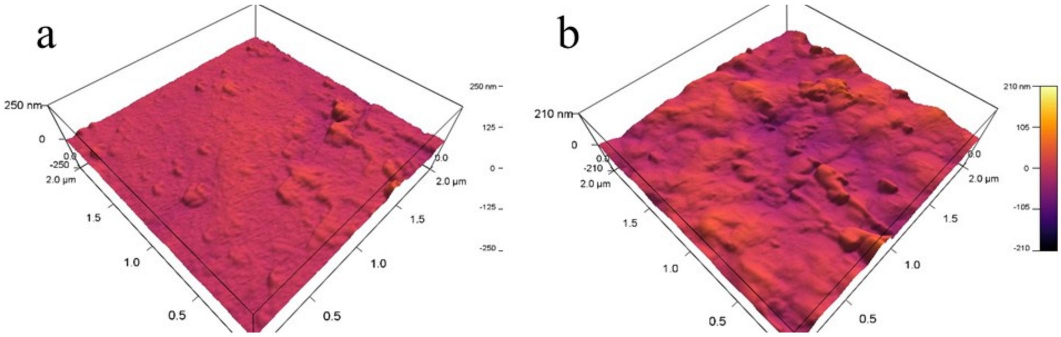

Figure S8 AFM morphology of Hydrogel-TFC membranes synthesized from PIP concentration of 0.0175 wt% and 0.02 wt%.

Table S1 Roughness of Hydrogel-TFC membranes

Hydrogel-TFC Membranes	PIP-0.015	PIP-0.0175	PIP-0.02
Roughness (nm)	7.28	8.1	8.06

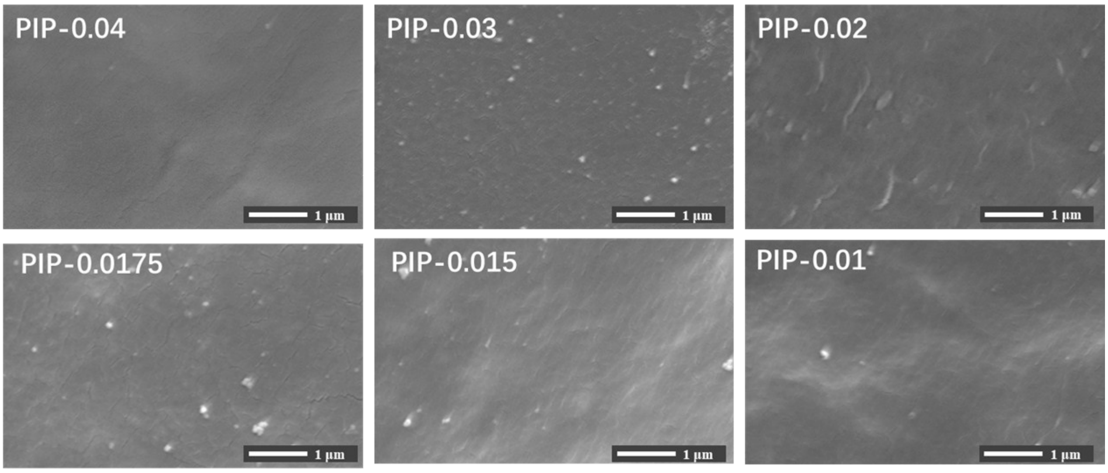

Figure S9 Surface morphology of Hydrogel-TFC membranes

Table S2 Elemental compositions and oxygen to nitrogen (O/N) ratios of Hydrogel-TFC membranes

Elements	C	N	O	O/N ratio
PIP-0.03wt%	70.26	9.50	20.24	2.13
PIP-0.02 wt%	68.74	9.5	21.76	2.29
PIP-0.0175 wt%	70.04	8.89	21.07	2.37
PIP-0.015 wt%	69.06	9.01	21.92	2.43

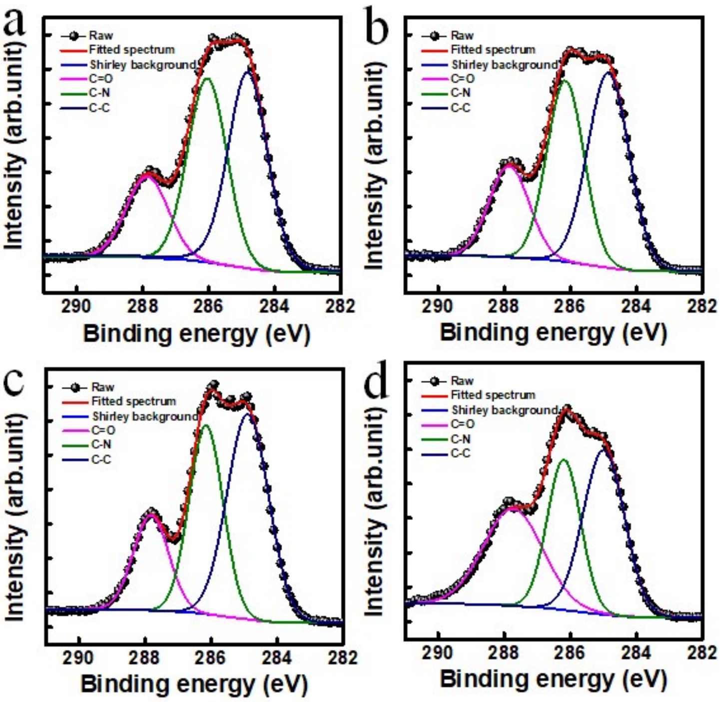

Figure S10 XPS narrow scan spectra of C 1s measured from the surfaces of Hydrogel-TFC membranes:

a, PIP-0.015 wt%, a, PIP-0.0175 wt%, a, PIP-0.02 wt%, a, PIP-0.03 wt%

Table S3 XPS results from Hydrogel-TFC membranes. Binding energies and plausible species were determined from the deconvolution of C1s, O1s and N1s core level XPS spectra.

Elements	Spices	Energy (ev)	0.015	0.0175	0.02	0.03
N 1s	C-NH-C	401	25.5	23.7	20.5	25.3
	C_2-N-C	400	74.4	76.3	79.5	74.7
O 1s	C-OH	532.5	58.9	63.0	65.4	78.7
	C=O	531	41.1	37	34.6	21.3
C 1s	C=O	287.8	18.1	19.8	18.4	33.4
	C-N	286	38.2	36.1	34.3	27.7
	C-C	284.8	43.8	44.1	47.3	38.8

Table S4 Rejection of different dyes in water by Hydrogel-TFC membranes

Dyes	Molecular weight (g mol^{-1})	PIP-0.0175 wt%	PIP-0.015 wt%
Congo red	697	99.9%	99.9%
Direct red 80	1373	99.7%	99.6%
Direct red 23	814	99.6%	99.1%
Reactive blue 2	774	98%	96%

2.3 PSU-TFC membranes

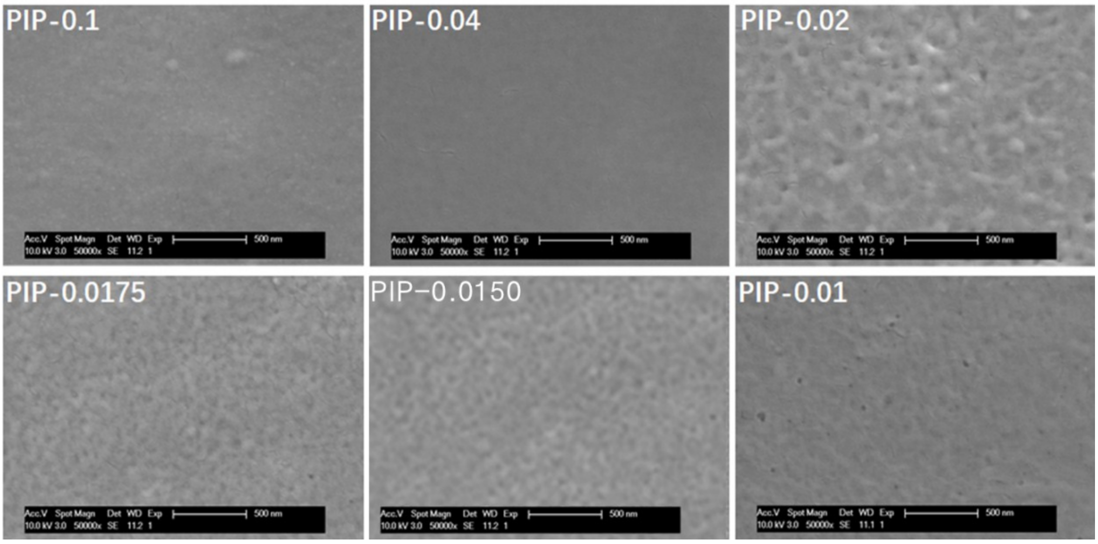

Figure S11 Surface morphology of PSU-TFC membranes

2.4 Freestanding-TFC membranes

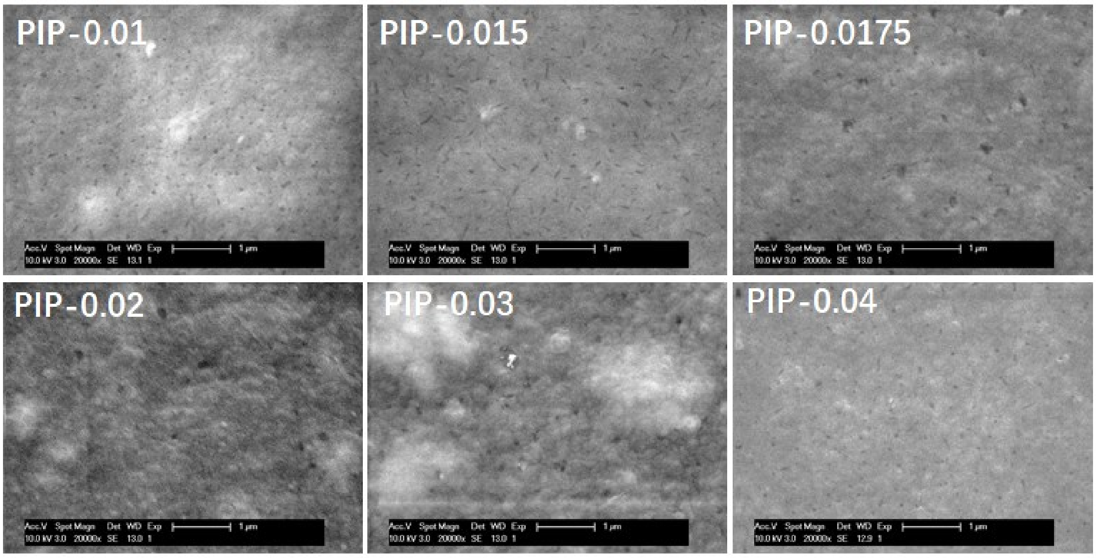

Figure S12 Surface morphology of Freestanding membranes

2.5 PVA based Hydrogel-TFC membrane

s

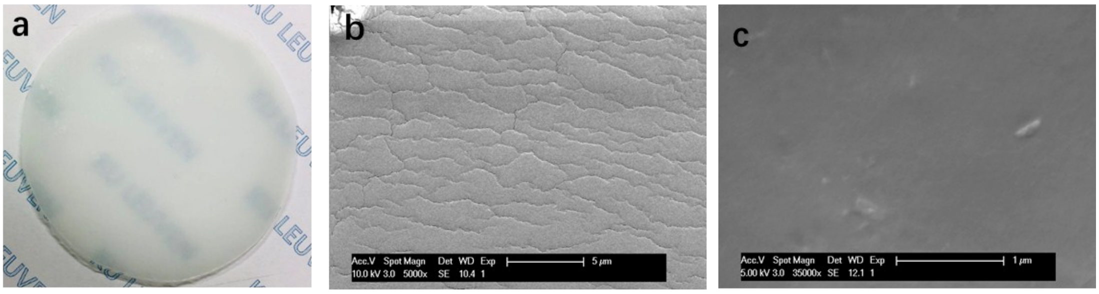

Figure S13 a Nonwoven supported PVA hydrogel membrane. b SEM image of PVA hydrogel surface. c Surface morphology of PVA Hydrogel-TFC membrane.

2.6 Comparison of hydrogel-TFC membranes, PSU-TFC membranes, and freestanding PA membranes

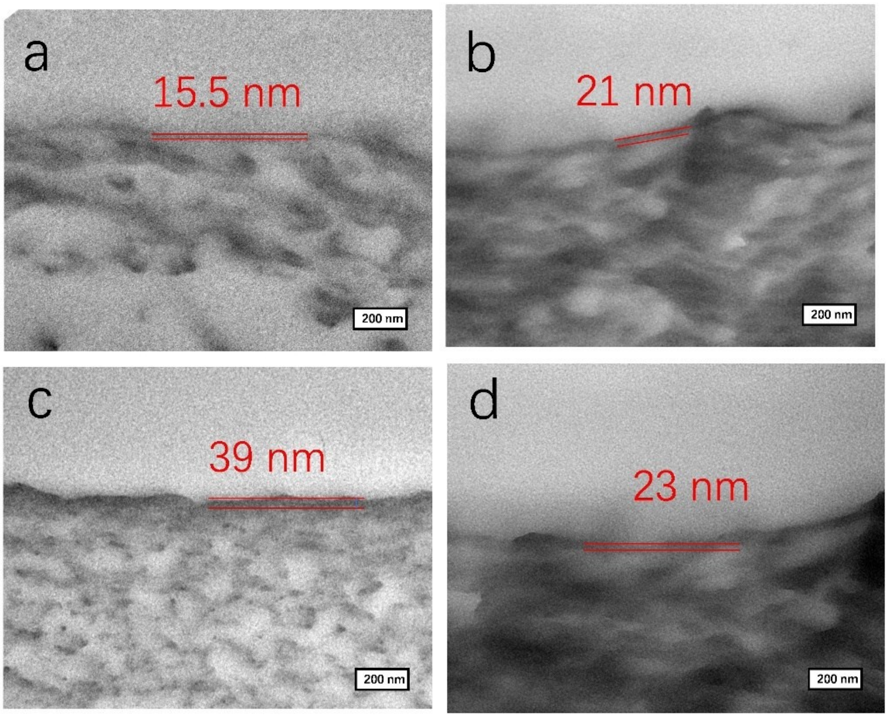

Figure S14 Thickness of the thin active layer. (a) hydrogel-TFC membrane synthesized using a PIP concentration of 0.015 wt%; (b) hydrogel-TFC membrane synthesized using a PIP concentration of 0.02 wt%; (c) hydrogel-TFC membrane synthesized using a PIP concentration of 0.04 wt%; (d) Freestanding membrane synthesized using a PIP concentration of 0.015 wt%.

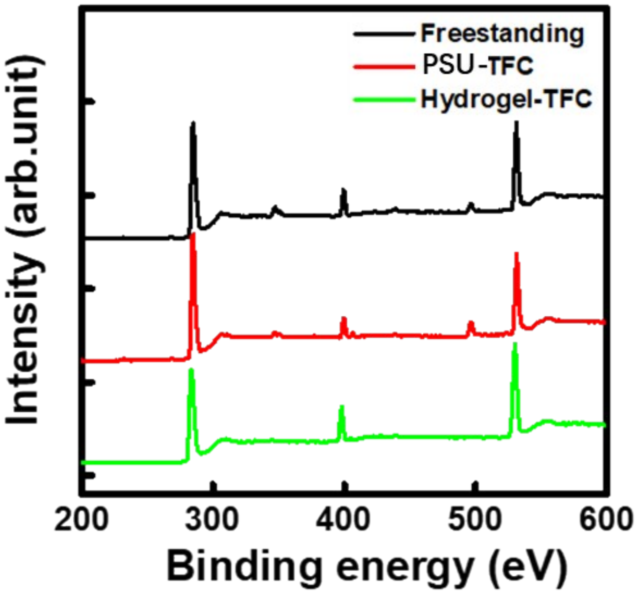

Figure S15 Chemical composition of freestanding PA membranes, PSU-TFC, and Hydrogel-TFC membranes.

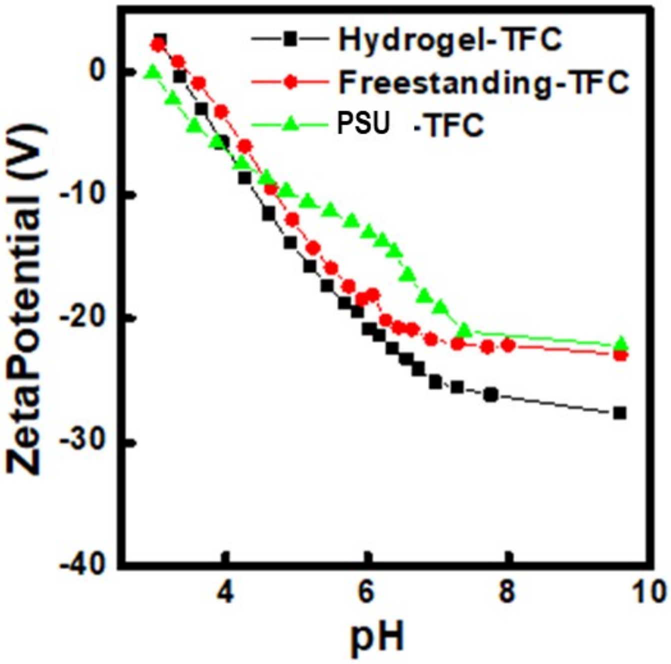

Figure S16 Zeta potential of freestanding PA membranes, PSU-TFC, and Hydrogel-TFC membranes (PIP: 0.015 wt%).

Table S5 Summary of the filtration performance of the state-of-the-art NF membranes reported in top 30 cited published papers in the last 3 years.

Number	Membranes	methods	Na_2SO_4 Rejection	Permeance	Surface	Ref.
	Hydrogel-TFC	IP	96.4	52.8	smooth	
	Hydrogel-TFC	IP	93.5	62.9	smooth	
1	COF	vacuum filtration	96.3	42.8	smooth	2
2	SWNCT/PA	IP	96.5	40	smooth	3
3	ZIF-8/PA	IP	93	14.3	rough	4
4	Cellulose	IP	97	34	smooth	5
5	TiO2@GO	IP	98.8	5.6	rough	6
6	SMWCNT	IP	96.8	13.2	smooth	7
7	SNW-1	IP	83.5	19.3	rough	8
8	Graphene oxide	electro-spraying	63.13	11.13	smooth	9
9	PA/GO-COCl	IP	97.1	22.6	rough	10
10	PDA/PEI	IP	97	7.5	smooth	11
11	PEI/PAA	Dopamine Deposition	96	8.7	smooth	12
12	ABA-PIP	IP	93.2	11.9	smooth	13
13	Sericin /PA	IP	97.5	16.4	smooth	14
14	PEA-TFC-NF	IP	96.27	6	smooth	15
15	PVDF-PAA/GO	vacuum filtration	79%	2.77	smooth	16
16	Dopamine/PIP	IP	90.5	14.5	smooth	17
17	SEPCMs	solution casting	93.4	6.42	smooth	18
18	Graphene oxide/IP	IP	95.8	3.4	rough	19

19	PA/PEG-POSS	IP	87.1	19.3	smooth	20
20	Dopamine	dopamine coating	81.2	10.29	smooth	21
21	PS/SiO_2	Layer by layer assembly	82.1	5	smooth	22
22	PAH/PAA	Layer by layer assembly	80	11.7	smooth	23
23	GO@nylon	Electrospinning, electrospraying	56.5	11.15	smooth	24
24	TFNMs	IP	97.8	10.6	rough	25
25	PA/MAH-GO	IP	97.6	8.22	smooth	26
26	PA/ATP	IP	92	22.95	smooth	27
27	PA/R-GO-NH2	IP	98.5	19.2	smooth	28
28	PA/PPTA	IP	98	7	smooth	29

3 Simulations

3.1 Molecular dynamics (MD) simulations

MD simulations were carried out to reveal the transport of PIP molecules by analyzing the generated trajectory frames in the pure water system and in the hydrogel system. All MD simulations were performed using the Forcite code in Materials Studio. A simulation box with periodic boundary conditions applied in all three dimensions was built in this work. Since in the experimental section, low PIP concentrations were used, the simulation box should be huge enough to allow several molecules of PIP to diffuse randomly in the system to obtain the same experimental concentration. However, this is time-consuming. Therefore, the concentration of PIP in MD simulation was manually adjusted for the convenience of calculation, and the simulation results can predict qualitative properties of the diffusion of PIP in the pure water/hydrogel system, as will be discussed in the following part. For the pure water system, a cubic simulation box with 21 Å side lengths was constructed, containing 320 H_2O molecules and 10 PIP molecules (corresponding to a concentration of 1.51 mol/L). While for the hydrogel system, the same numbers of H_2O and PIP molecules was inserted in the cubic box as in the pure water system, in addition to 2 repeat units of PPTA. The COMPASS force field was employed to account for the intermolecular interactions. Other simulation parameters were set according to the method used in a previous work. [30]

After the geometry optimization process of the system, the NVT ensemble followed by the NPT ensemble were applied in calculations with a time step of 1.0 fs and a total simulation time of 100 ps. Then the whole system was equilibrated for another 100 ps under NVT ensemble. The data were collected from the final 50 ps for analyzing. Frames containing the geometry information of the PIP molecules were output every 500 steps.

The mean square displacement (MSD) of PIP molecules in different systems was compared to investigate the mobility of PIP molecules in the system with or without the hydrogel. The diffusion coefficients of PIP molecules in different systems can be estimated from the slope of

MSD curves by Einstein relationship.[30]

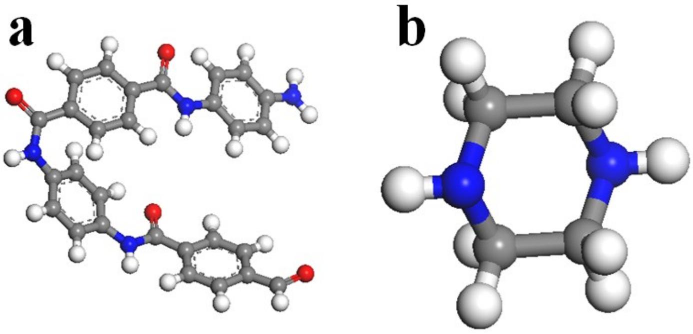

Figure S17 Chemical structure of Kevlar (two repeated units) and PIP used in MD simulation.

3.2 Dissipative particle dynamics (DPD) simulations

The theories of DPD simulations can be found in the literature. **[31, 32].** DPD simulations were carried out using the Mesocite module in Materials Studio to investigate the interfacial polymerization (IP) process of the PIP and TMC monomers at the n-hexane-water interface. Five different components were modeled in the IP system: water, PPTA, *n*-hexane, TMC and PIP. The coarse-graining level was defined with eight different beads (Table S6) and the repulsion parameters between DPD beads (Table S7) were calculated from Flory-Huggins parameters as reported previously.[33, 34]. In particular, the PPTA was included in water phase and compared with the system without hydrogel. In this study, a cubic simulation box of 100 × 100 × 100 $Å^3$ was constructed and divided into two slabs (100 × 100 × 50 $Å^3$) representing the n-hexane phase and the water phase, respectively. In the above slab, a layer of TMC beads mixed with *n*-hexane beads (*n*-hexane/TMC = 0.95: 0.05) were placed as the n-hexane phase. In the water phase, water, PIP and PPTA beads (water/PIP/PPTA = 0.85: 0.1: 0.05) were added in the bottom slab of the simulation box. To represent a stationary matrix of the hydrogel formed by PPTA molecules, all PPTA molecules in water phase were constrained on its motion, by fixing their positions during simulations. For comparison, pure water system without PPTA molecules were also constructed with the ratio water/PIP = 0.9 :0.1 in the water phase slab. The density of the whole system is 3 in reduced units. Each slab was independently equilibrated before the system was assembled for simulations.

Table S6 Coarse-grained structures for the components in the DPD systems of this work

Solvent	Chemical structure	Coarse-graining			Coarse-grained molecule
		Bead type	Molecular structure		
Water	H_2O	W	3 H_2O	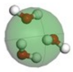	
PIP	$C_4H_{10}N_2$	M	CH_3OH	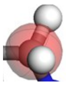	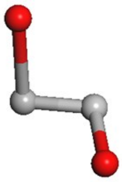
		D	$N(CH_3)_2$	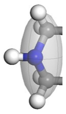	
Hexane	C_6H_{14}	H	C_6H_{14}	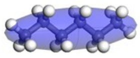	
TMC	$C_9H_3Cl_3O_3$	B	C_6H_6	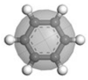	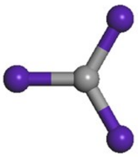
		C	CH_3COCl	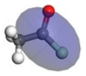	
PPTA	$(C_{14}H_{14}N_2O_4)_n$	E	C_8H_9NO	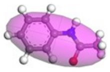	
		Z	C_7H_7NO	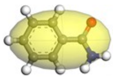	

Table S7 Conservative force parameter, a_{ij}, for the interacting beads

	B	C	D	E	H	M	W	Z
B	25.00							
C	25.07	25.00						
D	25.11	25.03	25.00					
E	36.15	33.40	32.76	25.00				
H	27.07	27.79	28.08	52.09	25.00			
M	36.11	33.23	74.07	25.48	51.28	25.00		
W	111.79	96.55	93.07	73.60	162.30	47.44	25.00	
Z	36.50	33.68	33.02	25.06	52.38	25.20	64.91	25.00

Based on the energy and temperature profiles, an initial period of 100 000 steps (15 ns) was left for equilibration of the system, and the simulation productions were carried out for an additional 400 000 steps (60 ns). IP interface configurations were extracted on the last 200 000 steps at every 500 steps. The snapshots of the initial simulation system before the IP process as well as the equilibrium state of the system after the IP process are presented. The descriptions of the hydrogel system are also presented to compare with the system without PPTA

4 Reference

1. J. Zhu, J. Hou, R. Zhang, S. Yuan, J. Li, M. Tian, P. Wang, Y. Zhang, A. Volodin and B. Van der Bruggen, *J. Mater. Chem. A*, 2018, **6**, 15701-15709.
2. H. Yang, L. Yang, H. Wang, Z. Xu, Y. Zhao, Y. Luo, N. Nasir, Y. Song, H. Wu and F. Pan, *Nature communications*, 2019, **10**, 2101.
3. S. Gao, Y. Zhu, Y. Gong, Z. Wang, W. Fang and J. Jin, *ACS nano*, 2019.
4. J. Zhu, L. Qin, A. Uliana, J. Hou, J. Wang, Y. Zhang, X. Li, S. Yuan, J. Li and M. Tian, *ACS Appl. Mater. Interfaces*, 2017, **9**, 1975-1986.
5. J.-J. Wang, H.-C. Yang, M.-B. Wu, X. Zhang and Z.-K. Xu, *J. Mater. Chem. A*, 2017, **5**, 16289-16295.
6. J. Wang, Y. Wang, J. Zhu, Y. Zhang, J. Liu and B. Van der Bruggen, *J. Membr. Sci.*, 2017, **533**, 279-288.
7. J. Zheng, M. Li, K. Yu, J. Hu, X. Zhang and L. Wang, *J. Membr. Sci.*, 2017, **524**, 344-353.
8. C. Wang, Z. Li, J. Chen, Z. Li, Y. Yin, L. Cao, Y. Zhong and H. Wu, *J. Membr. Sci.*, 2017, **523**, 273-281.
9. L. Chen, J.-H. Moon, X. Ma, L. Zhang, Q. Chen, L. Chen, R. Peng, P. Si, J. Feng and Y. Li, *Carbon*, 2018, **130**, 487-494.
10. P. Wen, Y. Chen, X. Hu, B. Cheng, D. Liu, Y. Zhang and S. Nair, *J. Membr. Sci.*, 2017, **535**, 208-220.
11. X. Yang, Y. Du, X. Zhang, A. He and Z.-K. Xu, *Langmuir*, 2017, **33**, 2318-2324.
12. Y. Chen, F. Liu, Y. Wang, H. Lin and L. Han, *J. Membr. Sci.*, 2017, **537**, 407-415.
13. M. B. M. Y. Ang, Y.-L. Ji, S.-H. Huang, H.-A. Tsai, W.-S. Hung, C.-C. Hu, K.-R. Lee and J.-Y. Lai, *J. Membr. Sci.*, 2017, **539**, 52-64.
14. Y. Pan, R. Xu, Z. Lü, S. Yu, M. Liu and C. Gao, *J. Membr. Sci.*, 2017, **523**, 282-290.
15. R. Zhang, S. Yu, W. Shi, W. Wang, X. Wang, Z. Zhang, L. Li, B. Zhang and X. Bao, *J. Membr. Sci.*, 2017, **542**, 68-80.
16. F. Baskoro, C.-B. Wong, S. R. Kumar, C.-W. Chang, C.-H. Chen, D. W. Chen and S. J. Lue, *J. Membr. Sci.*, 2018, **554**, 253-263.
17. J. Zhu, S. Yuan, A. Uliana, J. Hou, J. Li, X. Li, M. Tian, Y. Chen, A. Volodin and B. Van der Bruggen, *J. Membr. Sci.*, 2018, **554**, 97-108.
18. C.-C. Ye, F.-Y. Zhao, J.-K. Wu, X.-D. Weng, P.-Y. Zheng, Y.-F. Mi, Q.-F. An and C.-J. Gao, *Chem Eng J*, 2017, **307**, 526-536.
19. G. Lai, W. Lau, P. Goh, A. Ismail, Y. Tan, C. Chong, R. Krause-Rehberg and S. Awad, *Chem Eng J*, 2018, **344**, 524-534.
20. X. You, T. Ma, Y. Su, H. Wu, M. Wu, H. Cai, G. Sun and Z. Jiang, *J. Membr. Sci.*, 2017, **540**, 454-463.
21. Y. Chen and C. He, *Desalination*, 2017, **413**, 29-39.
22. W. Ding, H. Zhuo, M. Bao, Y. Li and J. Lu, *Chem Eng J*, 2017, **330**, 337-344.
23. S. Ilyas, S. M. Abtahi, N. Akkilic, H. D. W. Roesink and W. M. de Vos, *J. Membr. Sci.*, 2017, **537**, 220-228.
24. L. Chen, Y. Li, L. Chen, N. Li, C. Dong, Q. Chen, B. Liu, Q. Ai, P. Si and J. Feng, *Chem Eng*

J, 2018, **345**, 536-544.

25. Y.-L. Ji, Q.-F. An, X.-D. Weng, W.-S. Hung, K.-R. Lee and C.-J. Gao, *J. Membr. Sci.*, 2018, **548**, 559-571.
26. Q. Xie, W. Shao, S. Zhang, Z. Hong, Q. Wang and B. Zeng, *RSC Advances*, 2017, **7**, 54898-54910.
27. M. Wu, T. Ma, Y. Su, H. Wu, X. You, Z. Jiang and R. Kasher, *J. Membr. Sci.*, 2017, **544**, 79-87.
28. X. Li, C. Zhao, M. Yang, B. Yang, D. Hou and T. Wang, *Appl. Surf. Sci.*, 2017, **419**, 418-428.
29. Q. Shi, L. Ni, Y. Zhang, X. Feng, Q. Chang and J. Meng, *J. Mater. Chem. A*, 2017, **5**, 13610-13624.
30. L. Yao, Z. Qin, Q. Chen, M. Zhao, H. Zhao, W. Ahmad, L. Fan and L. Zhao, *Separation and Purification Technology*, 2018, **205**, 48-57.